Synthesis and Characterization of an Ultramicroporous Cesium Hydrogen Salt of 12-Tungstophosphoric Acid, $Cs_{2.1}H_{0.9}PW_{12}O_{40}$

Takashi Yamada, Yusuke Yoshinaga, and Toshio Okuhara*

Graduate School of Environmental Earth Science, Hokkaido University, Sapporo 060-0810

(Received May 14, 1998)

An ultramicroporous heteropoly compound, $Cs_{2.1}H_{0.9}PW_{12}O_{40}$, was synthesized by a titration method using aqueous solutions of $H_3PW_{12}O_{40}$ and Cs_2CO_3. Concentrations of the starting materials and the drop rate of Cs_2CO_3 solution were determined to synthesize $Cs_{2.1}H_{0.9}PW_{12}O_{40}$ having nearly uniform micropores and very low external surface area. The Dollimore-Heal method of N_2 isotherms showed that $Cs_{2.1}H_{0.9}PW_{12}O_{40}$ prepared by the controlled conditions has no mesopores. Adsorption of various molecules having different sizes revealed that the micropore size of $Cs_{2.1}H_{0.9}PW_{12}O_{40}$ was in the range from 0.43 to 0.59 nm and the fraction of the external surface area was less than 3% of the total surface area. A model for the unique ultramicropores has been proposed on the basis of the pore size, pore volume, and the primary crystallite size, in which the ultramicropores are spaces formed between the crystal faces of the mcirocrystallites as the primary particles of $Cs_{2.1}H_{0.9}PW_{12}O_{40}$.

Inorganic porous materials typified by zeolites are of great importance because of their potential for applications as adsorbents, catalysts, and sensors. Control of structure and width of their pores is keenly desirable for wider applications. Recently, new types of zeolite having unique pores such as ZSM-5,[1] VPI-5,[2] $AlPO_4$-8,[3] and UTD-1[4] have been synthesized. ZSM-5 is an excellent solid acid catalyst and has commercially been used for alkylation,[5] methanol to gasoline process,[6] and hydration.[7] Besides these zeolites, novel porous materials like mesoporous silica (MCM-41[8] and FSM-16[9]) and a variety of porous oxides, mixed oxides, and layered compounds have been reported.[10—14] Some of them have exhibited shape selectivities for various reactions.[12—14]

Heteropolyacids have high catalytic performances in a variety of reactions.[15—20] Several industrial processes utilizing these heteropoly compounds have operated.[21] The acid strength of $H_3PW_{12}O_{40}$ can be classified into superacidity.[22—24] Calorimetry of pyridine titration for acetonitrile solutions of various acids showed that $H_3PW_{12}O_{40}$ had a higher acid strength than that of H_2SO_4.[25] If the heteropolyacids are endowed with porosity, the resulting porous heteropoly compounds will be prominent catalysts, exhibiting shape selectivity.

Some porous heteropoly compounds have been known. Gregg et al.[26] found that ammonium salts of $H_3PW_{12}O_{40}$ and $H_3PMo_{12}O_{40}$ were porous. Mizuno and Misono[27] reported that stoichiometric cesium salts of $H_3PW_{12}O_{40}$ and $H_3PMo_{12}O_{40}$ possess mesopores which correspond to interparticle voids between the primary particles. On the other hand, Moffat et al.[28,29] inferred by analysis of N_2 adsorption–desorption isotherms and ^{129}Xe NMR that alkaline salts such as cesium salts and potassium salts are microporous. Okuhara et al.[23,30] claimed that some cesium hydrogen salts of $H_3PW_{12}O_{40}$ ($Cs_xH_{3-x}PW_{12}O_{40}$) were porous, and the pore width can be controlled by the content of Cs. Particularly, it was demonstrated that $Cs_{2.1}H_{0.9}PW_{12}O_{40}$ and $Cs_{2.2}H_{0.8}PW_{12}O_{40}$ are microporous, and $Cs_{2.5}H_{0.5}PW_{12}O_{40}$ possesses both micropores and mesopores.[23] Micropores and mesopores are defined as pores having widths smaller than 2 nm and 2—50 nm, respectively.[31]

Inumaru et al.[32,33] showed that the aggregates consisting of microcrystallites of $(NH_4)_3PW_{12}O_{40}$ were highly porous, where microcrystallites were connected to each other by epitaxial interfaces. More recently, Hölderich et al.[34] inferred from X-ray analysis that a salt of Dawson-type tungstophosphoric acid ($H_6P_2W_{18}O_{62}$) with hexamethylenediamine contains micropores in the crystal structure, while adsorption measurement did not give evidence for the presence of such pores.

In the present study, we attempted to establish the preparation conditions for microporous $Cs_{2.1}H_{0.9}PW_{12}O_{40}$ with uniform pores and to elucidate the microstructure and pore width. To determine the micropore-width, we measured the adsorption of various molecules having different sizes (we called this the "molecular-probe method"). In addition, the pore-size distribution in the mesopore region was analyzed by DH method[35] of N_2 adsorption–desorption isotherm. By comparison of the data with those for various zeolites, characteristics of the Cs salt were manifested.

Experimental

Preparation of samples. $H_3PW_{12}O_{40}$ supplied from the Nippon Inorganic Color and Chemical Co., Ltd. was purified by diethylether extraction. The aqueous solution of $H_3PW_{12}O_{40}$ was evaporated at 318 K to form a solid. The obtained $H_3PW_{12}O_{40}\cdot 13H_2O$ was evacuated at 338 K for 4 h to get $H_3PW_{12}O_{40}\cdot 6H_2O$. Cesium carbonate (Merck, extra pure) was

evacuated at 473 K for 4 h in a high vacuum system. The $H_3PW_{12}O_{40}\cdot 6H_2O$ and Cs_2CO_3, together with Milli-Q ultrapure water (Millipore), were used for preparation of each aqueous solution.

Cesium hydrogen salts, $Cs_{2.1}H_{0.9}PW_{12}O_{40}$ and $Cs_{2.5}H_{0.5}PW_{12}O_{40}$ (abbreviated as Cs2.1 and Cs2.5, respectively), were prepared by a titration method.[23] To the aqueous solution of $H_3PW_{12}O_{40}$, the aqueous solution of Cs_2CO_3 was added dropwise with vigorous stirring at room temperature. The concentrations of $H_3PW_{12}O_{40}$ and Cs_2CO_3 were in the ranges 0.02—0.08 mol dm^{-3} and 0.025—0.10 mol dm^{-3}, respectively. In addition, the drop rate of the Cs_2CO_3 solution was changed from 0.1 ml min^{-1} to 10.0 ml min^{-1} to reveal the influence on the porosity of the resulting solids. From the beginning of the addition of Cs_2CO_3, a white milky solution formed. The resulting colloidal solution was allowed to stand overnight at room temperature, and was then evaporated at 318 K to form a solid. Prior to use, these Cs salts were pretreated at 523 K in vacuum for 2 h.

As reference, H-ZSM-5 (HSZ-860HOA, Tosoh Co., 410 m^2 g^{-1}), $AlPO_4$-5 (synthesized by the method described in the literature,[36] 313 m^2 g^{-1}), HY (JRC-Z-HY 4.8, Reference Catalyst of Catalysis Society of Japan, 607 m^2 g^{-1}), NaY (HSZ-320NAA, Tosoh Co., 723 m^2 g^{-1}) were used after the evacuation at 673 K for 6 h. SiO_2 (Aerosil 300, Nippon Aerosil, 313 m^2 g^{-1}) was pretreated at 573 K in vacuum for 4 h.

Adsorption–Desorption Isotherms of N_2. N_2 adsorption–desorption isotherm was measured by an adsorption system (BELSORP 28SA, BEL Japan Inc.) at liquid nitrogen temperature. Pore size distribution in the range of mesopores was derived from the desorption branch of the N_2 isotherm by the DH method.[35]

Molecular Probe Method. Adsorption amounts of various kind of molecules having different sizes; *n*-butane, isobutane, benzene, CCl_4, 1,3,5-trimethylbenzene (abbreviated as TMB), and 1,3,5-triisopropylbenzene (abbreviated as TIPB), were measured with a microbalance (an improved TG-30, Shimadzu Co.) connected directly to a high vacuum system.[37] About 30 mg of Cs salt or 10 mg of H-ZSM-5, $AlPO_4$-5, HY, NaY or SiO_2 was set in a Pt pan, and was pretreated in vacuum under the above conditions. The relative pressure, p/p_0, was adjusted to 0.2, where p_0 is the saturated vapor pressure at the adsorption temperature. The adsorption was performed at 193 K for *n*-butane and isobutane, and at 298 K for benzene, CCl_4, TMB, and TIPB, respectively. The adsorption amount was measured after the adsorption reached nearly the equilibrium, which was attained at least after 1 h.

Other Measurements. Surface area was estimated from the N_2 isotherm by the BET method. XRD pattern was obtained by using Rigaku Geigerflex 2027 (monochromated Cu $K\alpha$).

Results

Effects of Preparation Conditions on Porosity. To establish the preparation conditions for a microporous cesium hydrogen salt $Cs_{2.1}H_{0.9}PW_{12}O_{40}$ (Cs2.1) having uniform pores, the effects of the concentrations and the rate of drop on the isotherm were first examined. Figure 1 shows the isotherms of N_2 adsorption–desorption for Cs2.1 by different $H_3PW_{12}O_{40}$ concentrations (0.02—0.08 mol dm^{-3}), where the concentration and the drop rate of the Cs_2CO_3 solution were adjusted to 0.1 mol dm^{-3} and 1.0 ml min^{-1}, respectively. All Cs2.1's obtained gave Type I isotherms. Type I isotherm is ordinarily observed for microporous materials.[38]

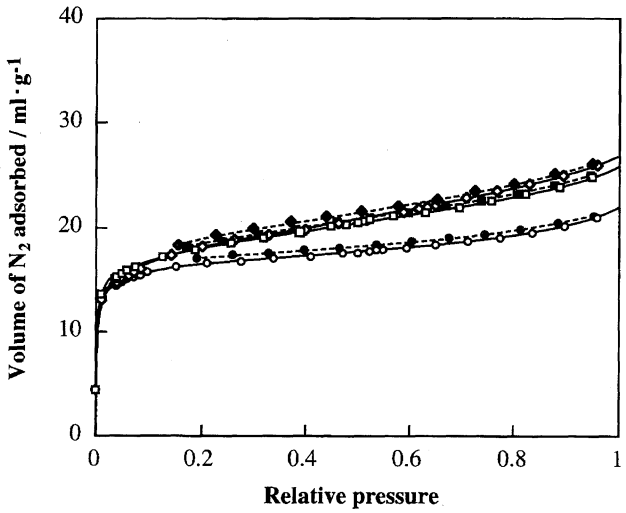

Fig. 1. N_2 adsorption–desorption isotherms at 77 K for $Cs_{2.1}H_{0.9}PW_{12}O_{40}$ prepared by different concentrations of $H_3PW_{12}O_{40}$. The concentration of $H_3PW_{12}O_{40}$: (◇, ◆); 0.02 mol dm^{-3}, (□, ■); 0.04 mol dm^{-3}, (○, ●); 0.08 mol dm^{-3}. Open and closed symbols are adsorption and desorption branches, respectively. The concentration of Cs_2CO_3 is 0.10 mol dm^{-3} and the drop rate is 1.0 ml min^{-1}.

The increase in the concentration from 0.02 to 0.08 mol dm^{-3} caused a downward shift of the isotherm, while the shape of the isotherm was almost unchanged. Consequently, the slope of the plateau became smaller at the concentration of 0.08 mol dm^{-3}.

Effects of the concentration of Cs_2CO_3 are given in Fig. 2. In this series, the concentration of $H_3PW_{12}O_{40}$ and the drop rate of Cs_2CO_3 solution were adjusted to 0.08 mol dm^{-3} and 1.0 ml min^{-1}, respectively. The N_2 isotherms for these

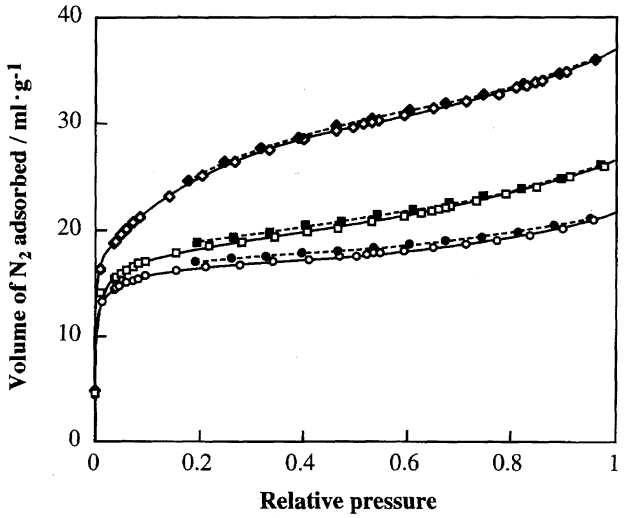

Fig. 2. N_2 adsorption–desorption isotherms at 77 K for $Cs_{2.1}H_{0.9}PW_{12}O_{40}$ prepared by different concentrations of Cs_2CO_3. The concentration of Cs_2CO_3: (◇, ◆); 0.025 mol dm^{-3}, (□, ■); 0.05 mol dm^{-3}, (○, ●); 0.1 mol dm^{-3}. Open and closed symbols are adsorption and desorption branches, respectively. The concentration of $H_3PW_{12}O_{40}$ is 0.08 mol dm^{-3} and the drop rate is 1.0 ml min^{-1}.

Cs2.1's were also classified into Type I isotherm. As the concentration of Cs_2CO_3 increased, the isotherm shifted downward. As a result, the slope of the plateau became smaller as the concentration of Cs_2CO_3 increased.

The drop rate of Cs_2CO_3 solution was also influential on the shape of isotherm. As the drop rate decreased from 10.0 to 0.1 ml min^{-1}, the isotherm shifted downward, as shown in Fig. 3. It is noted that the slope of plateau became nearly zero at the lowest drop rate (0.1 ml min^{-1}). As will be discussed below, the slope of plateau in the isotherm is related to the external surface area. Thus it is considered that the Cs2.1 prepared with $H_3PW_{12}O_{40}$ (0.08 mol dm^{-3}) and Cs_2CO_3 (0.1 mol dm^{-3}) and at the drop rate of 0.1 ml min^{-1} has the smallest external surface area. Hereafter, Cs2.1 prepared by the above conditions will be denoted as Cs2.1(s).

Figure 4 gives N_2 isotherms for zeolites and Cs2.5. H-ZSM-5, HY, and NaY gave Type I isotherms, and $AlPO_4$-5 and Cs2.5 Type IV isotherms. The hysteresis loops were observed for $AlPO_4$-5 and Cs2.5, indicating the presence of mesopores. In addition, the steep increases at very low pressures (p/p_0 <0.05) for $AlPO_4$-5 and Cs2.5 are consistent with the conclusion that these materials are also microporous. The isotherms of N_2 adsorption–desorption for $H_3PW_{12}O_{40}$ and SiO_2 are provided in Fig. 5. Typical Type II isotherms which are usually observed for nonporous materials[38] were observed for them.

Analysis of Pores of $Cs_{2.1}H_{0.9}PW_{12}O_{40}$. The pore volume of Cs2.1(s) was estimated both from *t*-plots[38] and Dubinin–Radushkevich plots.[39] Figure 6 shows *t*-plots of Cs2.1(s) and the Cs2.1 which has the highest capacity of N_2 adsorption (in Fig. 2, ◇, ◆), the latter being denoted to Cs2.1(h). Since the C_{BET} constant for Cs2.1(s) was very large (>1000), the interaction between the adsorbate and adsorbent would be rather strong. Sing et al.[38] recommend that a *t*-plot should be based on an isotherm of a non-porous reference material which is chemically similar to a sample. Thus, instead of a standard isotherm on SiO_2, we used the N_2 isotherm for $H_3PW_{12}O_{40}$ (shown in Fig. 5) as the standard

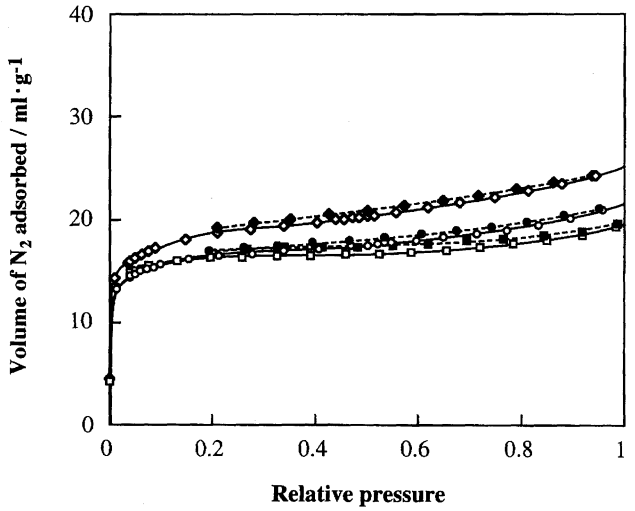

Fig. 3. N_2 adsorption–desorption isotherms at 77 K for $Cs_{2.1}H_{0.9}PW_{12}O_{40}$ prepared by different drop rates. The rate of drop: (□, ■); 0.1 ml min^{-1}, (○, ●); 1.0 ml min^{-1}, (◇, ◆); 10.0 ml min^{-1}. Open and closed symbols are adsorption and desorption branches, respectively. The concentration of $H_3PW_{12}O_{40}$ and Cs_2CO_3 are 0.08 and 0.10 mol dm^{-3}, respectively.

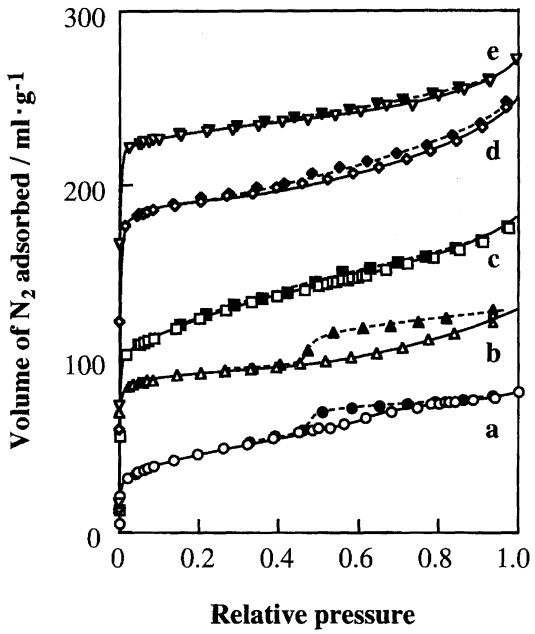

Fig. 4. N_2 adsorption–desorption isotherms of Cs2.5, $AlPO_4$-5 and zeolites at 77 K. a; Cs2.5 (S_{BET} = 135 $m^2 g^{-1}$), b; $AlPO_4$-5 (313 $m^2 g^{-1}$), c; H-ZSM-5 (410 $m^2 g^{-1}$), d; HY (607 $m^2 g^{-1}$), e; NaY (723 $m^2 g^{-1}$). Open symbols and closed symbols are adsorption and desorption branches, respectively.

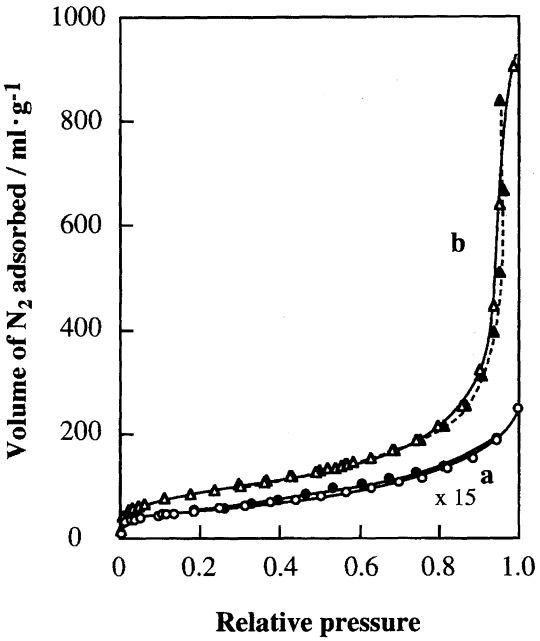

Fig. 5. N_2 adsorption–desorption isotherms of a; $H_3PW_{12}O_{40}$ (S_{BET} = 7 $m^2 g^{-1}$) and b; SiO_2 (313 $m^2 g^{-1}$) at 77 K. Open symbols and closed symbols are adsorption and desorption branches, respectively.

isotherm for *t*-plot.

In the *t*-plot (Fig. 6), Cs2.1(s) and Cs2.1(h) have knees at t = about 0.4, and each plot can be arranged by each straight line. The micropore volumes (in the unit of liquid nitrogen volume) of Cs2.1(s) and Cs2.1(h) were estimated from the intercepts of the ordinate to be 23.8 and 45.0 $mm^3\ g^{-1}$, respectively. Furthermore, the slopes of the two lines for Cs2.1(s) gave the total surface area by the micropores (65 $m^2\ g^{-1}$) and the external surface area (3 $m^2\ g^{-1}$), respectively. In the case of Cs2.1(h), the total surface area and the external surface area were determined to be 90 and 9 $m^2\ g^{-1}$, respectively.

Figure 7 provides a Dubinin–Radushkevich plot (DR plot)[39] for the N_2 adsorption for Cs2.1(s). According to the Dubinin–Radushkevich equation, the plot of $\log_{10} W$ against $\log^2_{10}(p_0/p)$ would give a straight line; the intercept on the ordinate corresponds to the total micropore volume (W_0), where W is the volume that has been filled at pressure p.[38,39] From the intercept of the straight line (Fig. 7), the micropore volume of Cs2.1(s) was determined to be 25.0 $mm^3\ g^{-1}$, which is close to that given by the *t*-plot (Fig. 6).

Figure 8 gives the mesopore size-distribution curves derived from the desorption branch of the N_2 isotherms by DH method.[35] Mesopores are defined as pores having a width from 2 to 50 nm.[31] It was shown that Cs2.5 has mesopores with the width of about 4.0 nm. Contrary to Cs2.5, no mesopore was detected for Cs2.1(s), while a small amount of the mesopores was observed for Cs2.1(h). $AlPO_4$-5, H-ZSM-5, and HY gave clear peaks due to mesopores of which the widths were 3.5—4.0 nm. As was not shown in this figure, SiO_2 had no peak due to mesopores.

Since it is difficult to estimate the pore size in the mi-

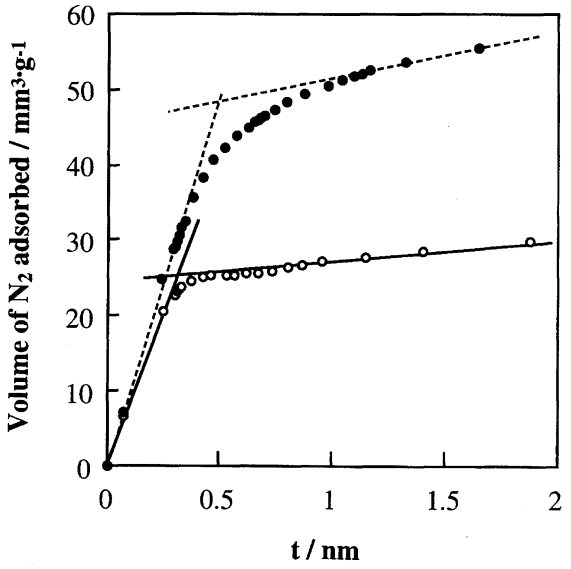

Fig. 6. The *t*-plots of $Cs_{2.1}H_{0.9}PW_{12}O_{40}$ prepared by different conditions. ○; Cs2.1(s); concentrations of $H_3PW_{12}O_{40}$ and Cs_2CO_3 were 0.08 and 0.1 mol dm^{-3}, and drop rate was 0.1 ml min^{-1}, ●; Cs2.1(h); concentrations of $H_3PW_{12}O_{40}$ and Cs_2CO_3 were 0.08 and 0.025 mol dm^{-3}, and drop rate was 1.0 ml min^{-1}.

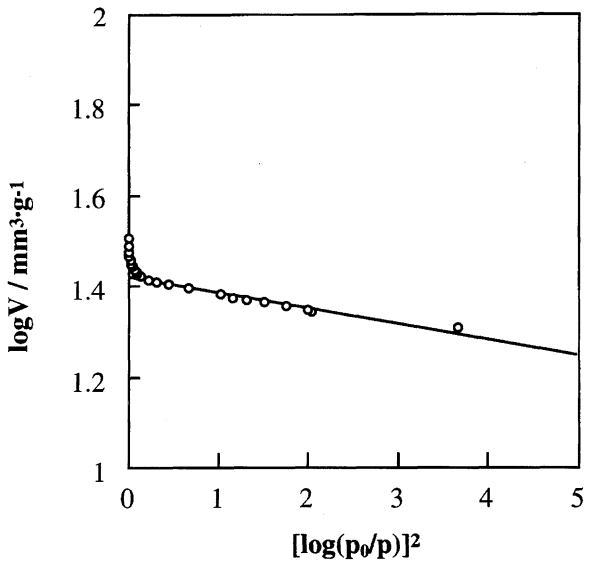

Fig. 7. Dubinin–Radushkevich plot for adsorption of N_2 isotherms of $Cs_{2.1}H_{0.9}PW_{12}O_{40}$ prepared by standard conditions (Cs2.1(s)).

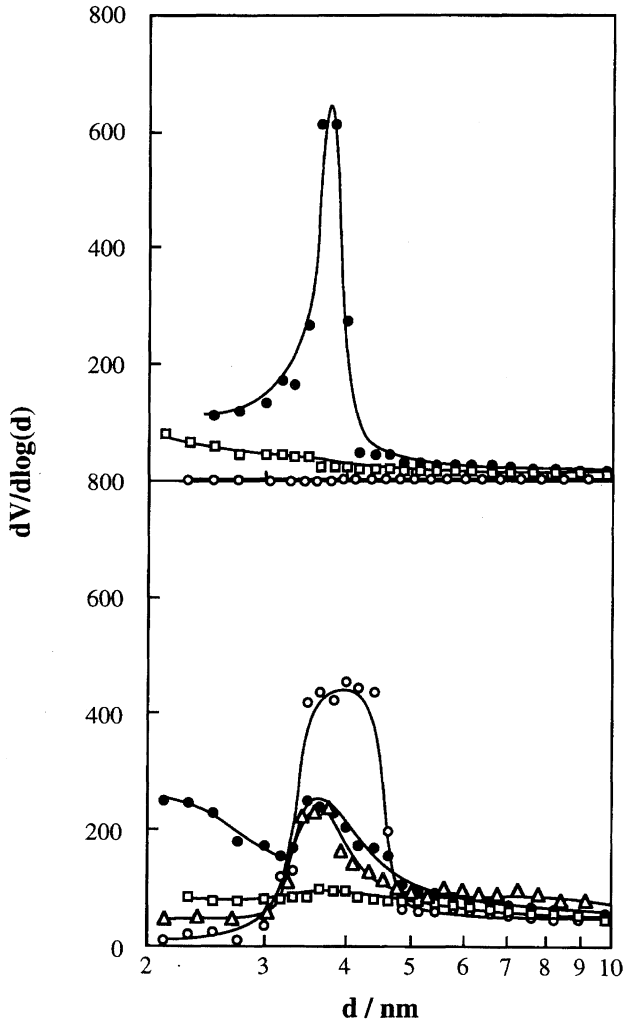

Fig. 8. Pore size distribution curves by Dollimore–Heal method. The upper: ○; Cs2.1(s), □; Cs2.1(h), ●; Cs2.5. The bottom: ○; $AlPO_4$-5, □; NaY, ●; H-ZSM-5, △; HY.

cropore region from the N_2 isotherm, another method is required. In the present study, the adsorption of various kinds of molecules was measured. Typical time courses of benzene adsorption are shown in Fig. 9. The adsorption amounts of benzene on these solids became constant within a few minutes. While appreciable amounts of benzene were adsorbed on NaY, HY, H-ZSM-5, and Cs2.5, it was clear that the adsorption on Cs2.1(s) was negligibly small.

The adsorption amounts of various molecules are summarized in Table 1. The molecular sizes are as follows:[40,41] N_2 0.36 nm, *n*-butane 0.43 nm, isobutane 0.50 nm, benzene 0.59 nm, CCl_4 0.59 nm, 1,3,5-trimethylbenzene 0.75 nm, and 1,3,5-triisopropylbenzene 0.85 nm. The "adsorption area" in the parentheses in Table 1 corresponds to the sum of the molecular cross sections of the total molecules adsorbed. This value was calculated from the molecular cross section A_m (nm^2) and the adsorption amount ($\mu mol\ g^{-1}$). The value of A_m was calculated from Eq. 1,[37] where M is the molecular weight, N is Avogadro's number, and d is the density of the molecules in the liquid state ($g\ nm^{-3}$):

$$A_m = 1.091(M/Nd)^{2/3}. \quad (1)$$

As is listed in Table 1, the BET surface area of Cs2.1(s) is 57 $m^2\ g^{-1}$ which is about half that of Cs2.5. The adsorption amount of *n*-butane on Cs2.1(s) was about half that of N_2 in the units of the adsorption area. Furthermore, the adsorption amount of isobutane was about 1/4 that of *n*-butane on Cs2.1(s). It should be noted that benzene and the other larger molecules were little adsorbed on Cs2.1(s). The "adsorption areas" of these molecules larger than benzene were less than 2% of the BET surface area by N_2. Contrary to Cs2.1(s), Cs2.5 has a large adsorption capacity for benzene (621 $\mu mol\ g^{-1}$) and other molecules. It was confirmed that for other porous solids like NaY, HY, $AlPO_4$-5, and H-ZSM-5, the adsorption area of benzene was more than 58% of the BET surface area.

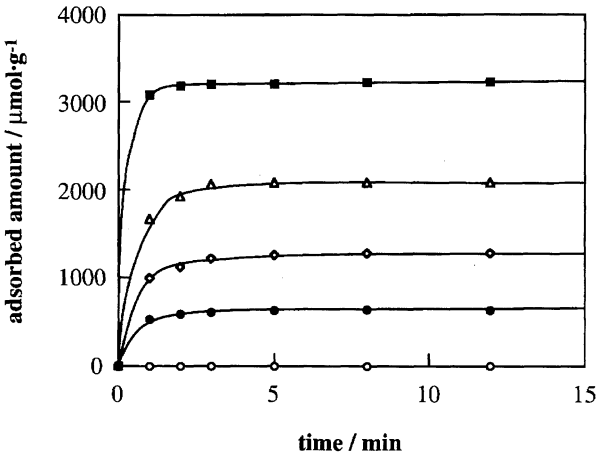

Fig. 9. Adsorption time course of benzene at 298 K. ○; Cs2.1, ●; Cs2.5, ◇; H-ZSM-5, △; HY, ■; NaY.

On H-ZSM-5 (channel size = 0.53×0.56 nm[1]), the "adsorption area" greatly decreased as the molecular size increased. Although TMB and TIPB were adsorbed on H-ZSM-5, the adsorption areas for TMB and TIPB were only 20 and 14% of the BET surface area, respectively. In the case of $AlPO_4$-5 (pore size 0.73 nm), the adsorption amount of TIPB was confirmed to be very low as compared with those of the other molecules. HY and NaY (pore size about 0.74 nm) readily adsorb the molecules smaller than TMB. However, the rate of adsorption of TIPB on HY and NaY was very slow, which is consistent with the results reported by Davis et al.[2] Table 1 showed that all of these molecules were adsorbed considerably on non-porous SiO_2, while the adsorption area was dependent on the kind of molecule.

Discussion

Preparation Conditions for Microporous $Cs_{2.1}H_{0.9}PW_{12}O_{40}$. Type I isotherms of N_2 for Cs2.1 (Figs. 1—3) indicate that these Cs2.1's are microporous. However, the pore-size distribution and the fraction of the external surface area depended greatly on the preparation conditions. Particularly, the concentration of Cs_2CO_3 solution was greatly influential. Cs2.1(s) which was prepared under the "standard conditions" gave a nearly flat plateau in the isotherm at the intermediate pressures (Fig. 3). Generally the increase in the adsorption amount at intermediate pressures is due to the multilayer adsorption.[38] Thus in the case of porous materials, the slope of the plateau is closely related to the external surface area.

The external surface area of Cs2.1(s) estimated from the *t*-plot (Fig. 6) was 3 $m^2\ g^{-1}$, which is only 4.5% of the total surface area (65 $m^2\ g^{-1}$). The total surface area of Cs2.1(s)

Table 1. Adsorption Data of Molecular Probe Method

Probe molecule	Adsorption amount[a]/$\mu mol\ g^{-1}$						
(diameter/nm)	Cs2.1	Cs2.5	H-ZSM-5	$AlPO_4$-5	HY	NaY	SiO_2
N_2[b] (0.36)	584 (57)	1384 (135)	4203 (410)	3167 (313)	6222 (607)	7442 (723)	3208 (313)
n-Butane (0.43)	135 (26)	681 (132)	2029 (394)	1126 (219)	3004 (583)	3294 (640)	909 (177)
Isobutane (0.50)	39 (8)	559 (108)	1715 (332)	1067 (206)	2768 (535)	3345 (647)	922 (179)
Benzene (0.59)	10 (2)	621 (114)	1303 (239)	1175 (216)	2600 (477)	3216 (590)	694 (127)
CCl_4 (0.59)	5 (1)	526 (102)	899 (174)	1988 (165)	1988 (385)	2260 (429)	463 (90)
TMB[c] (0.75)	6 (2)	442 (102)	278 (70)	516 (130)	1709 (429)	1935 (486)	854 (215)
TIPB[d] (0.85)	3 (1)	229 (82)	158 (56)	31 (11)	783[e] (279)	630[e] (224)	438 (156)

a) The figures in the parentheses show adsorption areas ($m^2\ g^{-1}$). b) Estimated from BET surface area ($m^2\ g^{-1}$). c) 1,3,5-trimethylbenzene. d) 1,3,5-triisopropylbenzene. e) Due to very slow adsorption, adsorption amounts were measured at 6 h.

is slightly larger than that of BET analysis, 57 $m^2 g^{-1}$. Since the BET surface area for microporous materials tends to be underestimated,[33] the above difference between the surface areas is reasonable. The external surface area of Cs2.1(h) was evaluated to be 9 $m^2 g^{-1}$ from the *t*-plot (Fig. 6) and corresponded to about 10% of that of the total surface area.

The results of the molecular probe method (Table 1) also support the smaller external surface area of Cs2.1(s). Benzene and the other larger molecules were little adsorbed on Cs2.1(s), demonstrating that the size of the micropores of Cs2.1 was less than 0.59 nm. The adsorption areas by these larger molecules on Cs2.1(s) were less than 2 $m^2 g^{-1}$ (Table 1), corresponding to 3% of the total surface area. This is consistent with the external surface area from the *t*-plot. The adsorption areas of TMB and TIPB for H-ZSM-5 used in the present study were 70 and 56 $m^2 g^{-1}$, respectively, indicating that the external surface area of H-ZSM-5 was more than 13% of the total surface area, while Take et al.[42] reported that the external surface area of a kind of H-ZSM-5 is 5% of the total surface area. Since the external surface of microporous materials affects unfavorably the shape selectivity, Cs2.1(s) is a promising candidate for the shape selective catalyst because of its very small external surface area. Actually, Pt-promoted Cs2.1 having the small external surface area exhibited an excellent reactant shape selectivity for hydrogenation and oxidation.[43]

For the microstructure of cesium hydrogen salts of $H_3PW_{12}O_{40}$, we proposed a model.[44] During the titration, microcrystallites of $Cs_3PW_{12}O_{40}$ having about 10 nm in diameter are first formed in the solution, and then these crystallites are thickly covered by $H_3PW_{12}O_{40}$ remaining in the solution.[23] Upon the evaporation, large aggregates (secondary particles) are formed and at the same time interparticle voids are generated.[23,45] The adduct of Cs3 and $H_3PW_{12}O_{40}$-overlayer has the composition of $Cs_2HPW_{12}O_{40}$ and its aggregates ($Cs_2HPW_{12}O_{40}$) obtained after the dryness are non-porous large particles. Probably the interstices between the primary particles are occupied by very small particles or amorphous phase acting as cements.[45] The micropores of Cs2.1 are probably interparticle voids between the primary crystallites. When the Cs content (Cs/polyanion) exceeded 2, the salts became porous and the pore width increased as the Cs content increased. The crystallite size (by XRD) of Cs3 itself was about 10 nm and the particle size estimated from the surface area was 7 nm. That is, the crystallite size is comparable with the particle size, which means that Cs3 consists of fine non-porous crystallites. On the other hand, in the case of Cs2, the particle size (about 1000 nm) is very much larger than the crystallite size (about 12 nm). Therefore, the secondary particles of Cs2 must be non-porous large aggregates consisting of fine crystallites.

If so, the rate of the growth of the Cs3 cores and the formation of the adduct with $H_3PW_{12}O_{40}$-overlayer may be influential for the pore structure. Considering the mechanism for the formation of pores, the formation of Cs3 core as the primary crystallites is probably critical for uniform micropores. As given in Fig. 2, as the concentration of Cs_2CO_3 increased, narrower distributions of the pores and lower fractions of the external surface areas were obtained. Probably the rate for the growth of the Cs3 crystallites became faster as the Cs_2CO_3 concentration increased, which might lead to the uniform distribution of the size of Cs3 cores. The drop rate of Cs_2CO_3 is likely to be related to the rate of growth of the Cs3 crystallites. As a matter of fact, the slower drop of Cs_2CO_3 solution was favorable for the lower fraction of the external surface area. This is also understood by the uniform growth of the Cs crystallites under the adequate concentration and drop rate. The other factors like the evaporation conditions to get the solid (temperature, rate, etc.) and drying conditions would also be influential for the pore structure, while these conditions were controlled carefully in the present study.

Formation of Micropores. The size of primary particles of Cs2.1(s) was estimated to be about 12 nm from the linewidth of XRD. The micropores of Cs2.1(s) are considered to be interparticle voids between the primary crystallites. The molecular probe method demonstrated that the pore size of Cs2.1(s) was in the range from 0.43 nm (corresponds to the size of *n*-butane) to 0.59 nm (the size of benzene). There are no such pores in the primary crystallites themselves,[27] where the crystallites consist of Keggin anion and Cs ion in bcc structure. If the defect sites of Cs ion are responsible for the pores, the pore-width would be less than the size of Cs ion, 0.34 nm. Furthermore, if the lack of Keggin anion caused the formation of pores, the pores would have the size of about 1.1 nm. Thus the above presumed pore sizes are not in accordance with the pores of Cs2.1(s) observed in the present study.

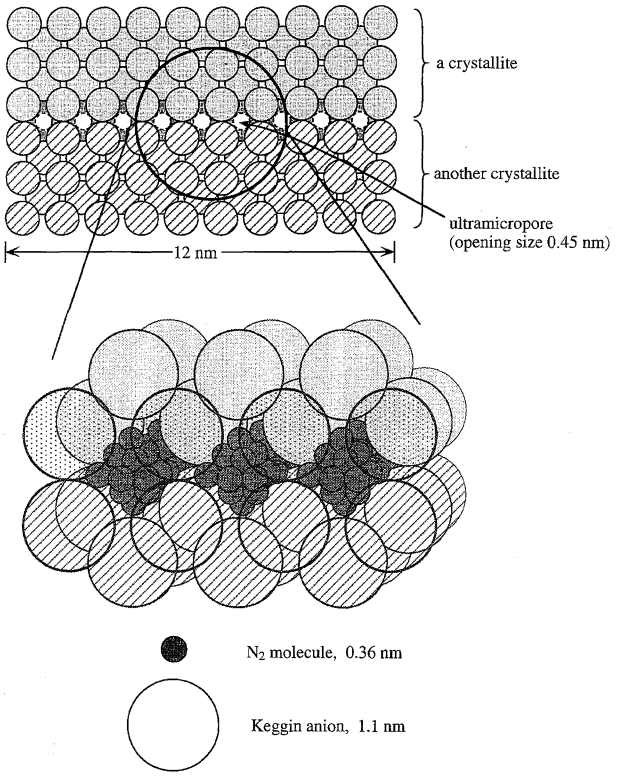

Fig. 10. A proposed model for micropores of $Cs_{2.1}H_{0.9}PW_{12}O_{40}$.

For the ultramicropores of Cs2.1(s), we propose the following model, shown in Fig. 10. We speculate that the micropores are spaces formed between the crystal faces of the primary crystallites, that is, the spaces correspond to voids formed by crystallographic mismatching. When the polyanion is assumed to be a rigid sphere having the diameter of 1.1 nm, the expected size of the pores formed by a possible arrangement of the crystal planes is 0.46—0.55 nm (Fig. 10).

Since the external surface area of Cs2.1 is 2 $m^2 g^{-1}$, the secondary particle size of this porous solid is estimated to be 545 nm in length from the density (5.5 $g cm^{-3}$). Assuming cubic shape particles, one may calculate that one gram of Cs2.1 contains 1.1×10^{12} of the secondary particles having the length of 545 nm. Considering the crystallite size of 12 nm, we find that one secondary particle consists of $45\times45\times45$ crystallites and contains $45\times45\times44\times3$ ($=2.6\times10^5$) contact faces between the crystallites. One contact face contains 9×9 pores and each pore corresponds to a space surrounded by 10 Keggin anions, as illustrated in Fig. 10. The value of one space is simply estimated to be 1.30 nm^3. Considering the diameter of N_2 molecule (0.36 nm), 16 molecules of N_2 can be incorporated in a pore. Therefore, the total amount of N_2 adsorbed in the pores of Cs2.1 is estimated to be $1.1\times10^{12}\times2.6\times10^5\times81\times16 = 3.9\times10^{20}$ molecules $= 6.5\times10^{-4}$ mol. By using the density of liquid N_2 (0.81 $g cm^{-3}$), the above adsorption amount of N_2 is converted to 22.5 mm^3 in the unit of N_2 liquid volume. This value is in good agreement with the experimental ones (23.8 and 25.0 $mm^3 g^{-1}$), suggesting that the pores are formed by mismatching of the crystal faces of the microcrystallites of $Cs_{2.1}H_{0.9}PW_{12}O_{40}$. Although at present, there is no direct evidence for shape of the micropores and the mechanism of the formation, we wish to emphasize that this material has nearly uniform pores and greatly depressed external surface area, and therefore is a promising candidate as a shape selective catalyst or its precursor.

Conclusion

The microporous heteropoly compound, $Cs_{2.1}H_{0.9}PW_{12}O_{40}$, was prepared by the controlled conditions and had only ultramicropores with the width of 0.43—0.59 nm. The external surface area was less than 3% of that of the total surface area. From the pore-width, pore volume, and the crystallite size of the primary particles, a unique model for the pores is proposed, in which the pores are formed between the crystal faces.

This study was partly supported by a Grant-in-Aid for Scientific Research No. 9555243 from the Ministry of Education, Science, Sports and Culture. Kawasaki Steel 21st Century Foundation is gratefully acknowledged. The authors thank Dr. Ryuichiro Ohnishi (Catalysis Research Center, Hokkaido University) for preparation of $AlPO_4$-5.

References

1) G. T. Kokotailo, S. L. Lawton, D. H. Olson, and W. M. Meier, *Nature*, **272**, 437 (1978).
2) M. E. Davis, C. Saldarriga, C. Montes, J. Gardes, and C. Crowder, *Nature*, **331**, 698 (1998).
3) R. M. Dessau, J. L. Schlenker, and J. B. Higgins, *Zeolites*, **10**, 522 (1990).
4) C. C. Freyhardt, M. Tsapatsis, R. F. Lobo, K. J. Balkus, Jr., and M. E. Davis, *Nature*, **381**, 295 (1996).
5) N. Y. Chen and W. E. Garwood, *Catal. Rev. -Sci. Eng.*, **28**, 185 (1986); N. Y. Chen, W. E. Garwood, and F. G. Dwyer, "Shape-Selective Catalysis in Industrial Application," 2nd ed, Mercel Dekker, New York (1996).
6) C. D. Chang, *Catal. Rev. -Sci. Eng.*, **25**, 1 (1983).
7) H. Ishida, Y. Fukuoka, O. Mitsui, and M. Kono, *Stud. Surf. Sci. Catal.*, **83**, 437 (1994).
8) J. S. Beck, J. C. Vartulli, W. J. Roth, M. E. Loenowincy, C. T. Kresge, K. D. Schmitt, C. T-W. Chu, D. H. Olsen, E. W. Sheppard, S. B. McCullen, J. B. Higins, and J. L. Schlenker, *J. Am. Chem. Soc.*, **114**, 10834 (1992).
9) S. Inagaki, Y. Fukushima, and K. Kuroda, *J. Chem. Soc., Chem. Commun.*, **1993**, 680.
10) M. Toba, F. Mizukami, S. Niwa, and K. Maeda, *J. Chem. Soc., Chem. Commun.*, **1990**, 1211.
11) W. F. Maier and P. A. Jacobs, *Angew. Chem., Int. Ed. Engl.*, **35**, 180 (1996).
12) S. Klein and W. F. Maier, *Angew. Chem., Int. Ed. Engl.*, **35**, 2230 (1996).
13) I. V. Kozhevnikov, A. Sinnema, R. J. Jansen, K. Pamin, and H. Van Bekkum, *Catal. Lett.*, **30**, 241 (1995).
14) A. Corma, *Chem. Rev.*, **97**, 2373 (1997).
15) T. Okuhara, N. Mizuno, and M. Misono, *Adv. Catal.*, **41**, 113 (1996).
16) M. Misono, *Catal. Rev. -Sci. Eng.*, **29**, 296 (1987).
17) Y. Izumi, K. Urabe, and M. Onaka, "Zeolites, Clay and Heteropoly Acid in Organic Reactions," Kodansha, Tokyo and VHC, Weinheim, New York (1992).
18) Y. Ono, "Perspectives in Catalysis," ed by J. M. Thomas and K. I. Zamaraev, Blackwell, London (1993), p. 341.
19) I. V. Kozhevnikov, *Chem. Rev.*, **98**, 171 (1998).
20) A. Corma, *Chem. Rev.*, **95**, 559 (1995).
21) M. Misono and N. Nojiri, *Appl. Catal.*, **64**, 1 (1990).
22) T. Okuhara, T. Nishimura, and M. Misono, *J. Mol. Catal.*, **74**, 247 (1992).
23) T. Okuhara, T. Nishimura, and M. Misono, *Stud. Surf. Sci. Catal.*, "11th Inter. Congr. Catal. —40th Aniversary," 1996, ed by J. W. Hightowerm, W. N. Delgass, E. Iglesia, and A. T. Bell, Elsevier, Amsterdam, Vol. 101, p. 581.
24) F. Lefevre, F. X. Liu-Cai, and A. Auroux, *J. Mater. Chem.*, **4**, 125 (1994).
25) R. S. Drago, J. A. Dias, and T. Maier, *J. Am. Chem. Soc.*, **119**, 7709 (1997).
26) S. T. Gregg and M. M. Tayyab, *J. Chem. Soc., Faraday Trans. 1*, **74**, 348 (1978).
27) N. Mizuno and M. Misono, *Chem. Lett.*, **1987**, 961.
28) J. B. MacMonagle and J. B. Moffat, *J. Colloid Interface Sci.*, **101**, 479 (1984).
29) J. L. Bonardet, J. Fraissard, G. B. McGarvey, and J. B. Moffat, *J. Catal.*, **151**, 147 (1995).
30) T. Okuhara, T. Nishimura, and M. Misono, *Chem. Lett.*, **1995**, 155.
31) J. Rouquerol, D. Avnir, C. W. Fairbridge, D. H. Everett, J. H. Haynes, N. Pernicone, J. D. F. Ramsay, K. S. W. Sing, and K. K. Unger, *Pure Appl. Chem.*, **66**, 1739 (1994).

32) K. Inumaru, H. Nakajima, T. Itoh, and M. Misono, *Chem. Lett.*, **1996**, 559.
33) T. Ito, K. Inumaru, and M. Misono, *J. Phys. Chem.*, **48**, 9958 (1997).
34) W. Höldrich, M. Hasse, and F. Näumann, *Angew. Chem., Int. Ed. Engl.*, **27**, 226 (1988).
35) D. Dollimore and G. R. Heal, *J. Colloid Interface Sci.*, **33**, 508 (1970).
36) E. M. Flanigen, B. M. Lok, R. L. Pattom, and S. T. Wilson, *Stud. Surf. Sci. Catal.*, **28**, 103 (1986).
37) K. Inumaru, T. Okuhara, and M. Misono, *J. Phys. Chem.*, **95**, 4026 (1991).
38) S. J. Gregg and K. S. W. Sing, "Adsorption, Surface area and Porosity," 2nd ed, Academic Press, London (1982).
39) M. M. Dubinin and L. V. Raduschkevich, *Proc. Acad. Sci. USSR*, **55**, 331 (1947).
40) D. W. Breck, "Zeolite Molecular Sieves," Wiley, New York (1974).
41) D. E. W. Vauham and R. J. Lussier, "Proc. 5th Intern. Conf. Zeolites," ed by L. V. C. Ree, Heyden & Sons, 1980, p. 94.
42) J. Take, H. Yoshioka, and M. Misono, "Proc. 9th Int. Congr. Catal.," The Chemical Institute of Canada, Ottawa, 1988, Abstr., Vol. 1, p. 372.
43) Y. Yoshinaga, K. Seki, T. Nakato, and T. Okuhara, *Angew. Chem., Int. Ed. Engl.*, **36**, 2833 (1997).
44) K. Na, T. Iizaki, T. Okuhara, and M. Misono, *J. Mol. Catal. A: Chem.*, **115**, 449 (1997).
45) T. Okuhara, T. Nishimura, H. Watanabe, and M. Misono, submitted for publication.